Timing of Quantal Release from the Retinal Bipolar Terminal Is Regulated by a Feedback Circuit

Michael A. Freed,* Robert G. Smith,
and Peter Sterling
Department of Neuroscience
University of Pennsylvania School of Medicine
Philadelphia, Pennsylvania 19104

Summary

In isolation, a presynaptic terminal generally releases quanta according to Poisson statistics, but in a circuit its release statistics might be shaped by synaptic interactions. We monitored quantal glutamate release from retinal bipolar cell terminals (which receive GABA-ergic feedback from amacrine cells) by recording spontaneous EPSCs (sEPSCs) in their postsynaptic amacrine and ganglion cells. In about one-third of these cells, sEPSCs were temporally correlated, arriving in brief bursts (10–55 ms) more often than expected from a Poisson process. Correlations were suppressed by antagonizing the $GABA_C$ receptor (expressed on bipolar terminals), and correlations were *induced* by raising extracellular calcium or osmolarity. Simulations of the feedback circuit produced "bursty" release when the bipolar cell escaped intermittently from inhibition. Correlations of similar duration were present in the light-evoked sEPSCs and spike trains of sluggish-type ganglion cells. These correlations were suppressed by antagonizing $GABA_C$ receptors, indicating that glutamate bursts from bipolar terminals induce spike bursts in ganglion cells.

Introduction

At an isolated presynaptic terminal, quantal release is generally a Poisson process (Barrett and Stevens, 1972; Del Castillo and Katz, 1954; Stevens, 1993), with a few exceptions (Abenavoli et al., 2002; Bornstein, 1978; Cohen et al., 1974). Yet a presynaptic terminal in the brain commonly participates in local feedback circuits that might shape the terminal's release statistics. This is especially worth considering because the statistics of quantal input to a neuron might shape the statistics of its spike output, which in turn determine its information capacity (de Ruyter van Stevenick et al., 1997; Kara et al., 2000; Meister and Berry, 1999).

To investigate whether local circuits shape quantal statistics, we analyzed temporal patterns of spontaneous and evoked release from retinal bipolar cells. These neurons transmit a graded potential down a short axon that releases glutamate at 30–130 active zones (Cohen and Sterling, 1990a; Tsukamoto et al., 2001). Each active zone is presynaptic to two processes, often a ganglion cell dendrite plus an amacrine cell process that releases GABA or glycine back onto the bipolar terminal (Figure 1; Grunert and Wassle, 1993; Hartveit, 1999; Koulen et al., 1998b). Because the bipolar synapse excites and

*Correspondence: michael@retina.anatomy.upenn.edu

the amacrine synapse inhibits, the circuit constitutes a negative feedback loop that might shape the statistics of bipolar cell release.

To monitor quantal release from bipolar terminals, we recorded spontaneous excitatory postsynaptic currents (sEPSCs) from ganglion or amacrine cells and constructed autocorrelograms of sEPSC times. Poisson-distributed events can appear bursty, because short intervals are more common than long ones; therefore, to quantify release statistics, we constructed autocorrelograms. For many cells, the autocorrelogram showed that EPSCs were temporally correlated into bursts, and thus departed from the temporal independence expected for a Poisson distribution.

Having found these temporal correlations, we investigated their origin by perturbing synaptic connections either pharmacologically or by ionic exchanges. To help interpret these experiments, parallel perturbations were made to a simulated feedback circuit. We also investigated whether temporal correlations reached the output stage of the retina by recording light-evoked responses from ganglion cells and constructing autocorrelograms of both quantal inputs and spike output. The results provide evidence that feedback circuitry in the inner retina shapes the statistics of the ganglion cell spike train.

Results

sEPSCs in Certain Cells Were Temporally Independent

We monitored the bipolar cell's spontaneous release by recording from ganglion and amacrine cells in a retinal slice preparation at room temperature (20°C–22°C) under a steady, bright light (<0.1% RMS noise). Spontaneous EPSCs were detected offline automatically (see Experimental Procedures). The peak amplitude was 9 ± 5 pA (mean $\pm$ SD), indicating a conductance of 100 ± 60 pS ($E_{glut} = 0$ mV, $V_{memb} = -87$ mV), the rise time was 0.6 ± 0.3 ms, and the decay time constant was 6 ± 6 ms (n = 51 cells). These events resembled previous descriptions (Protti et al., 1997; Taylor et al., 1995; Tian et al., 1998). Autocorrelograms were constructed to show arrival times, relative to a given sEPSC, of all *other* sEPSCs.

Autocorrelograms for about three-quarters of the cells in the ganglion cell layer (GCL, 66/87) and about half of the cells in the amacrine layer (ACL, 35/66) were flat with a notch near the origin (at $t = 0$, Figure 2A). To establish an interpretation for such plots, we studied three amacrine cells in more detail. First, sEPSCs were excised from a record and then shuffled and redistributed according to Poisson statistics. The mean rate of the Poisson process was adjusted until the rate of sEPSCs detected in the shuffled case equaled the rate of sEPSCs detected in the original recording. To match the original recording, intervals between sEPSCs were filled with noise (Gaussian, $\sigma = 0.3$–0.8 pA). Autocorrelograms of shuffled and original recordings matched: both
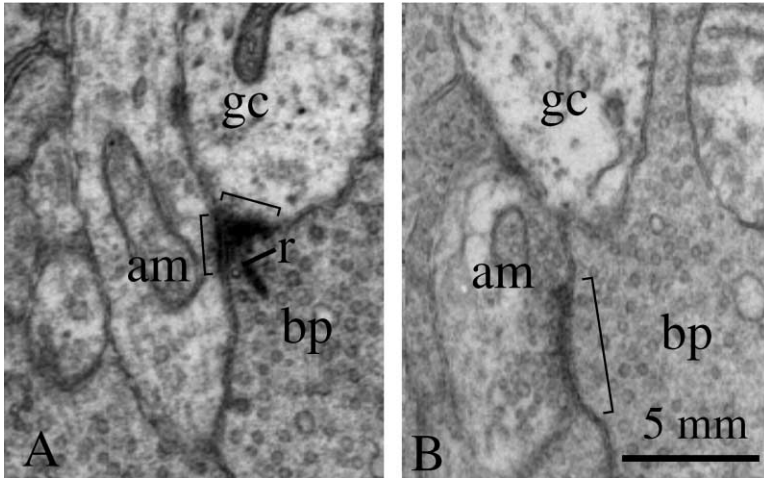
Figure 1. Bipolar Cell Axon Terminal Receives Feedback

(A) Bipolar synapse (bp) marked by a ribbon (r) contacts both a ganglion cell (gc) and an amacrine cell (am).

(B) Seven sections away (~0.6 μm), the same amacrine process feeds back onto the bipolar terminal. Brackets indicate active zones. Guinea pig retina prepared for electron microscopy by standard methods (Freed et al., 1987).

were flat with notches of equal depth. Thus, the autocorrelogram from the original recording was entirely consistent with independently timed events.

To establish whether the autocorrelogram was distorted by our detection algorithm, we constructed an autocorrelogram of *all* sEPSCs in the shuffled recording, both detected and undetected (unlike an actual recording, the times for all sEPSCs in the shuffled re-
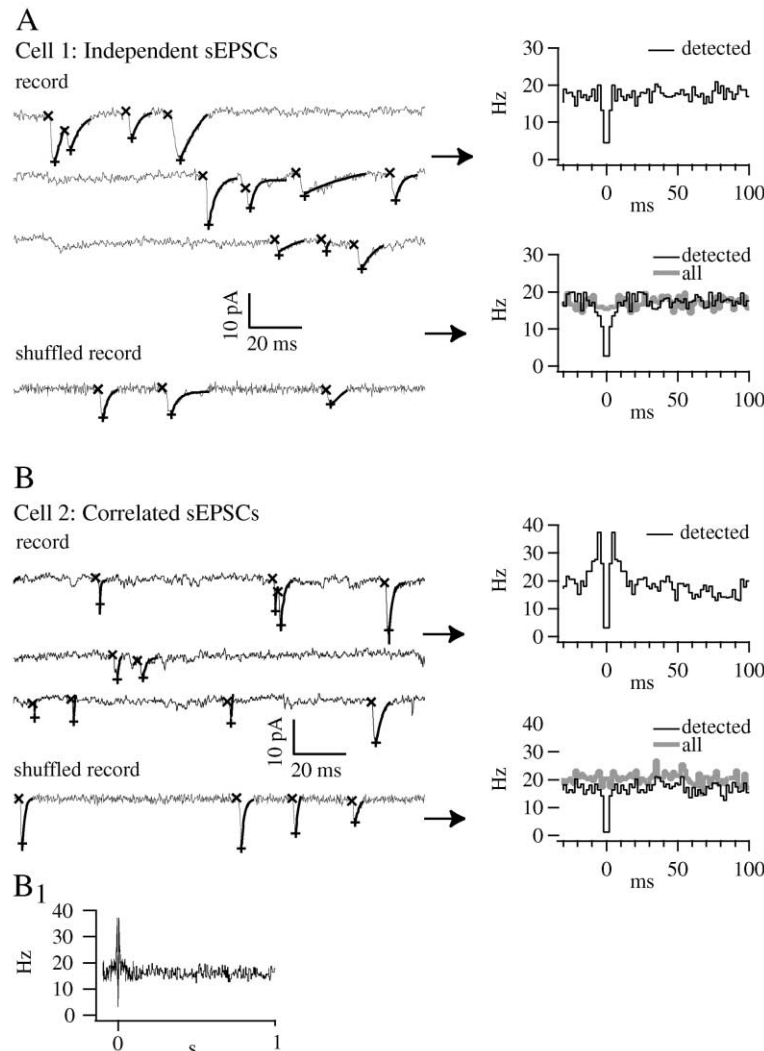

Figure 2. In Certain Neurons, sEPSC Arrived Independently, but in Others They Were Temporally Correlated

(A) Cell 1: whole-cell recordings were analyzed using a peak location algorithm that identifies sEPSCs by their leading edge (X), peak (+), and exponential decay (thick lines). The autocorrelogram of detected sEPSCs was flat except for an artifactual notch around the origin due to unreliable of detection of overlapped events. When sEPSCs were shuffled and their times reset according to Poisson statistics, the autocorrelogram of *detected* sEPSCs matched that from the original record. The autocorrelogram of *all* sEPSCs, both detected and undetected, was flat and lacked the notch.

(B) Cell 2: autocorrelogram from actual record had a positive peak. Peak disappeared when the events were shuffled and redistributed according to Poisson statistics.

(B$_1$) At longer time scale, autocorrelogram from cell 2 lacked secondary peaks; thus, correlated sEPSCs were not periodic.

cording were known). This autocorrelogram was also flat, but slightly higher than the autocorrelogram of detected sEPSCs (by 1–2 Hz), and it lacked a notch at the origin. Since these differences were due to the undetected sEPSCs, we reviewed undetected sEPSCs in the simulated recordings and found that most (~90%) followed a detected event so closely (within 3 ms) that the two were counted as a single event. Thus, there was a limit to the time resolution of the detection algorithm, which slightly depressed the autocorrelogram and introduced an artifactual notch, but otherwise the autocorrelogram's structure was undistorted.

sEPSCs in One-Third of Cells
Were Temporally Correlated

Autocorrelograms for about one-third (52/153) of cells showed a positive peak near the origin (Figure 2B). This included about one-quarter of the cells in the ganglion cell layer (GCL, 21/87) and about one-half of the cells in the amacrine cell layer (ACL, 31/66). Three such amacrine cells were analyzed as described above; that is, the sEPSCs were shuffled, redistributed according to Poisson statistics, and automatically detected in the synthetic record. This removed the autocorrelogram's original peak. Since the shuffled recording contained the same detected sEPSCs, the original peak could not have been an artifact of the detection algorithm interacting with sEPSC time course or amplitude (Clements and Bekkers, 1997). Instead, the peak genuinely indicated that sEPSCs were positively correlated.

We quantified the strength of correlation by calculating the proportion of sEPSCs that exceeded the expectation from a Poisson process. First, we calculated the integral of the autocorrelogram from $t = 0$ to the time where the peak subsided into the baseline and then calculated the fraction of this integral that rose above the baseline (Figure 3A). Correlation strength varied between cells, ranging from 2% to 68%, with a mean value of about 20% ± 15% (Figure 3B). There was no difference between ACL and GCL (p = .86). We also calculated the correlation duration as the time at which the peak in the autocorrelogram subsided into the baseline. Correlations lasted from 10 to 55 ms; cells in the ACL had slightly longer correlations than those in the GCL (25 ± 11 ms versus 18 ± 9 ms, p = .03).

Cells in the ACL produced recordings with lower noise than cells in the GCL, presumably because they had lower capacitance (7.6 ± 4 versus 11 ± 8 pF, p < 0.001) (Marty and Neher, 1995). Cells in the GCL include both ganglion and amacrine cells, but cells in the ACL are all amacrine cells. Thus, to maintain recording quality and to record from a single neuronal class, the following experiments were performed on amacrine cells in the ACL of retinal slices.

Antagonists of the Feedback Synapse
Suppressed sEPSC Correlations

If the correlated arrival of sEPSCs were caused by a feedback circuit (Figure 1), then blocking receptors postsynaptic to the inhibitory synapse should abolish or reduce correlations. To test this, we bath-applied antagonists of GABA$_A$, GABA$_C$, and glycine receptors and quantified the percent change in correlation

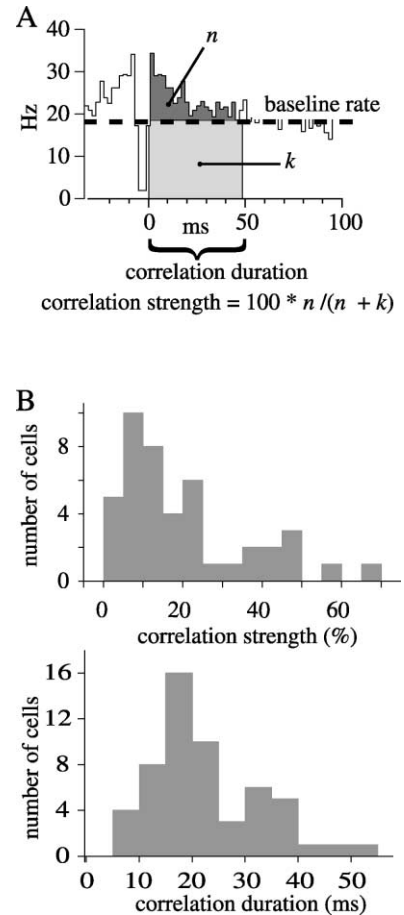$$\text{correlation strength} = 100 * n / (n + k)$$

Figure 3. Correlation Strength and Duration across Cells

(A) Correlation strength was measured as the proportion of the peak's integral that lies above the baseline; correlation duration was the time at which the peak subsides into the baseline.

(B) Distributions across cells of correlation strength and correlation duration.

strength and duration. We also performed null experiments, exchanging solutions without adding antagonist. All antagonist effects were compared to the effects of the null experiments to calculate their statistical significance (t test for uncorrelated samples assuming unequal variance, $\alpha = 0.05$).

Picrotoxin (80 μM), a combined GABA$_A$ and GABA$_C$ antagonist, consistently reduced correlation strength by 60% ± 20% (n = 4/4 cells, Figures 4A and 4C). TPMPA (1,2,5,6-tetrahydropyridin-4-yl methylphosphinic acid, 60 μM), a specific GABA$_C$ antagonist, also reduced correlation strength—and by a similar amount, 70% ± 30% (n = 7/7 cells). Both effects were significant (p < 0.01), and both effects reversed when recording time was sufficient for antagonist washout (~10 min; n = 5/5 cells) (McGillem et al., 2000). Bicuculline (30 μM), a specific GABA$_A$ antagonist, and strychnine (2 μM), a glycine antagonist, did not significantly effect correlation strength (n = 4 cells for each antagonist, p > 0.1). None of the antagonists altered the correlation duration (p > 0.1 for each antagonist, not shown). Thus, although bipolar terminals postsynaptic to amacrine synapses express
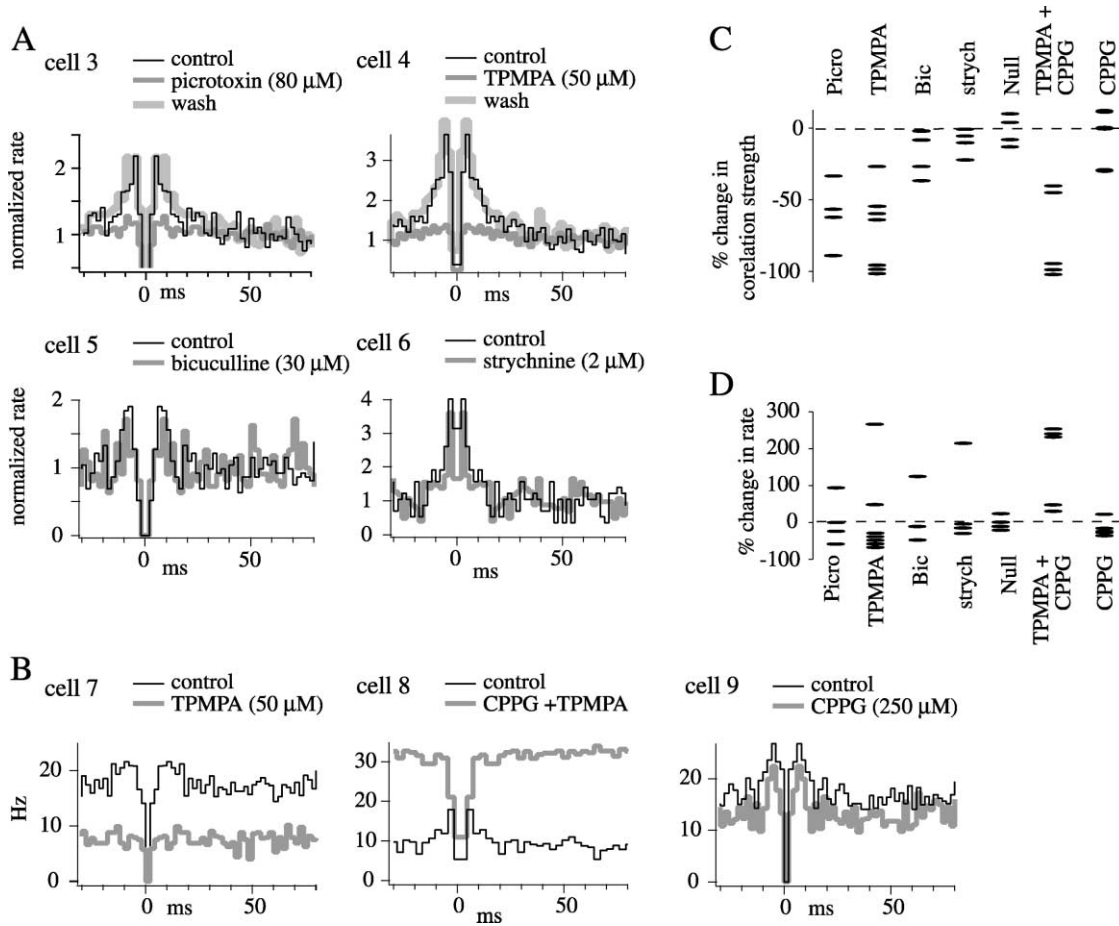
Figure 4. Antagonists of GABA_C Receptor Suppressed Correlations

(A) Picrotoxin and TPMPA (GABA_C antagonists) suppressed correlations, whereas bicuculline and strychnine (GABA_A and glycine antagonists) were ineffective. To show strength of correlations, autocorrelograms were divided by the baseline rate (normalized).

(B) TMPA alone often reduced the baseline rate, but combined with CPPG (mGluR antagonist), it invariably raised the baseline rate. CPPG alone did not affect rate. Autocorrelograms are not normalized.

(C and D) Antagonist effects across cells on correlation strength and baseline rate.

all three receptor types (Grunert and Wassle, 1993; Hartveit, 1999; Koulen et al., 1998b), the correlations were consistently suppressed only by antagonists of GABA_C. Possibly GABA_A and glycine receptors on the bipolar terminal localize postsynaptic to "nonreciprocal" amacrine processes (Fletcher and Wassle, 1999; Koulen et al., 1998a) and thus serve inhibitory mechanisms other than the feedback described here (e.g., Demb et al., 1999; Freed et al., 1987). Alternatively, they may provide feedback on bipolar cell types that do not produce correlated release.

The GABA_C antagonists did not always block correlations completely, possibly due to incomplete antagonism. Yet, because long recording times (~30 min) were required to construct autocorrelograms in control and drug conditions, we could not assess dosage effects on correlations and so chose a single effective concentration ($>K_d$) that avoided nonspecific effects (Chebib et al., 1998; McGillem et al., 2000; Picaud et al., 1998).

Combining Antagonists of Feedback Synapse and Autoreceptor Increased Release Rate

Because GABA and glycine antagonists reduce inhibition on the bipolar cell, they were expected to increase the baseline release rate. Unexpectedly, these antagonists often *reduced* the baseline rate (Figures 4B and 4D). A metabotropic glutamate receptor is located on the bipolar axon terminal and thus may supply negative feedback, which would suppress glutamate release (Awatramani and Slaughter, 2001) and thus prevent the expected rate increase. To test this idea, we applied the type III metabotropic glutamate antagonist CPPG ((RS)-α-cyclopropyl-4-phosphonophenylglycine, 250 μM). CPPG alone had no significant effect on correlation or rate (n = 5/5 cells, p > 0.3), indicating in agreement with Awatramani and Slaughter (2001) that the mGluR feedback circuit is not constitutively active (Figure 4B). CPPG might ordinarily suppress photoreceptor hyperpolarization of the On bipolar cell, thus increasing its
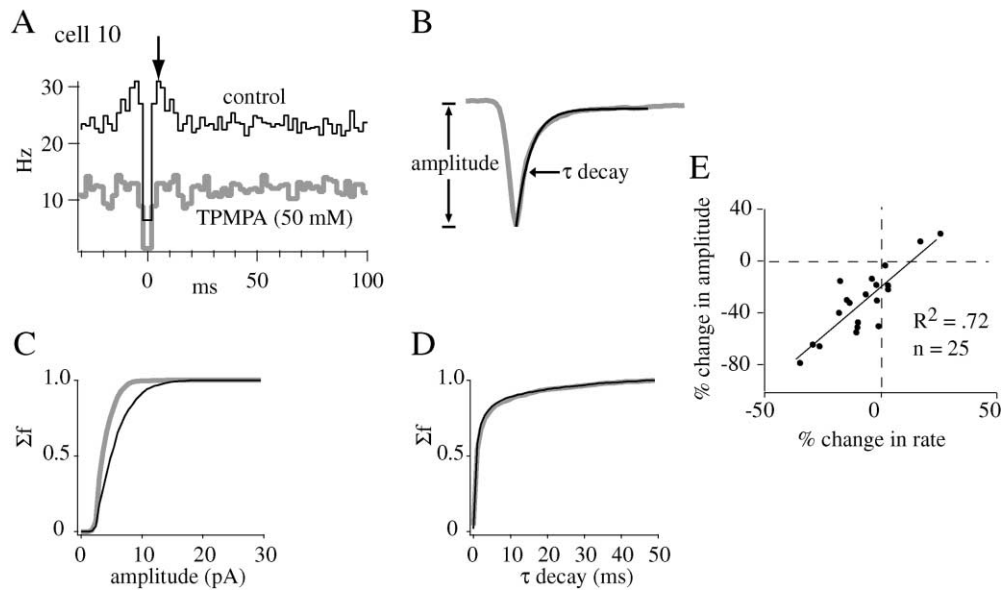
Figure 5. Evidence that GABA$_C$ Antagonist Reduces sEPSC Size by Desynchronizing Quanta

(A) TPMPA blocked sEPSC correlations. Arrow indicates sEPSC rate at short intervals (see text).

(B) Amplitude and the time constant of decay were measured in control and TPMPA solutions.

(C) TPMPA shifted the cumulative frequency distribution to smaller amplitudes.

(D) TPMPA did not affect cumulative frequency distribution of time constant.

(E) For 25 cells, the change in average sEPSC amplitude was correlated (in both antagonist and null experiments) with change in rate at short intervals. This suggests that antagonists reduce sEPSC size by reducing the frequency of coincident quanta.

release, but in the present experiments photoreceptor input was already curtailed by bright light. However, when CPPG was applied together with the GABA$_C$ antagonist, TPMPA, this combination suppressed the correlation (n = 5/5 cells, p < 0.003) and increased the baseline rate by 30% to 260% (n = 5/5 cells, p < 0.003). Thus, with the metabotropic glutamate receptor antagonized, suppressing inhibition did evoke the expected increase in baseline rate.

Evidence that Antagonists Reduced sEPSC Amplitude by Desynchronizing Quanta

To see if antagonists alter the shape of individual sEPSCs, we compared the amplitude and decay times of sEPSCs in control and antagonist solutions (Figure 5). The average time from baseline to peak was omitted because its measured value (0.6 ± 0.3 ms) was affected by the time constant of the recording system (~0.3 ms, see Experimental Procedures). We limited the analysis to picrotoxin and TPMPA because these antagonists had the greatest effects on correlation strength. The average decay time constant was 5 ± 4 ms in the control condition and did not change significantly when an antagonist was added (6 ± 4 ms, p = 0.4). The average amplitude in the control condition, 6 ± 2 pA, was mildly but significantly reduced by the antagonists to 5 ± 2 pA (n = 17 cells, p = 0.01).

If quanta coincide, they produce a larger sEPSC than if they occur singly; thus, antagonists might have reduced the sEPSC amplitude by desynchronizing quanta

(Protti et al., 1997; Tian et al., 1998). The frequency of coincident quanta is the autocorrelogram's value at $t = 0$, but because coincident sEPSCs were not detected, we estimated this value from the autocorrelogram's value just outside the notch (Figure 5A, arrow). Graphing this value against the percent change in sEPSC amplitude for all cells subject to an antagonist or to the null experiment (n = 25, Figure 5D), we found a correlation large enough to explain about 72% of the variation in sEPSC amplitude ($R^2 = 0.72$, p < 0.001). Thus, the data were consistent with the idea that antagonists decrease sEPSC amplitude by decreasing the frequency of coincident quanta.

Increasing External Calcium and Osmolarity Induced sEPSC Correlations

If sEPSC correlations are caused by synaptic feedback, then augmenting synaptic transmission in the feedback loop should enhance them. To test this idea, we augmented transmission by increasing external Ca^{2+} from 1.2 to 2.2 mM (substituting Ca^{2+} for Mg^{2+}, see Experimental Procedures); alternatively, we increased external osmolarity from 300 to 500 mOsm by adding 200 mM dextrose. Neither manipulation affected the correlation strength of cells that showed a correlation in the standard Ames' solution (n = 7/20, p = 0.65, not shown). Yet, both manipulations induced a correlation in most cells that initially lacked a correlation in standard solution (n = 16/20, Figures 6A–6C). For all cells recorded long enough to construct an autocorrelogram after a
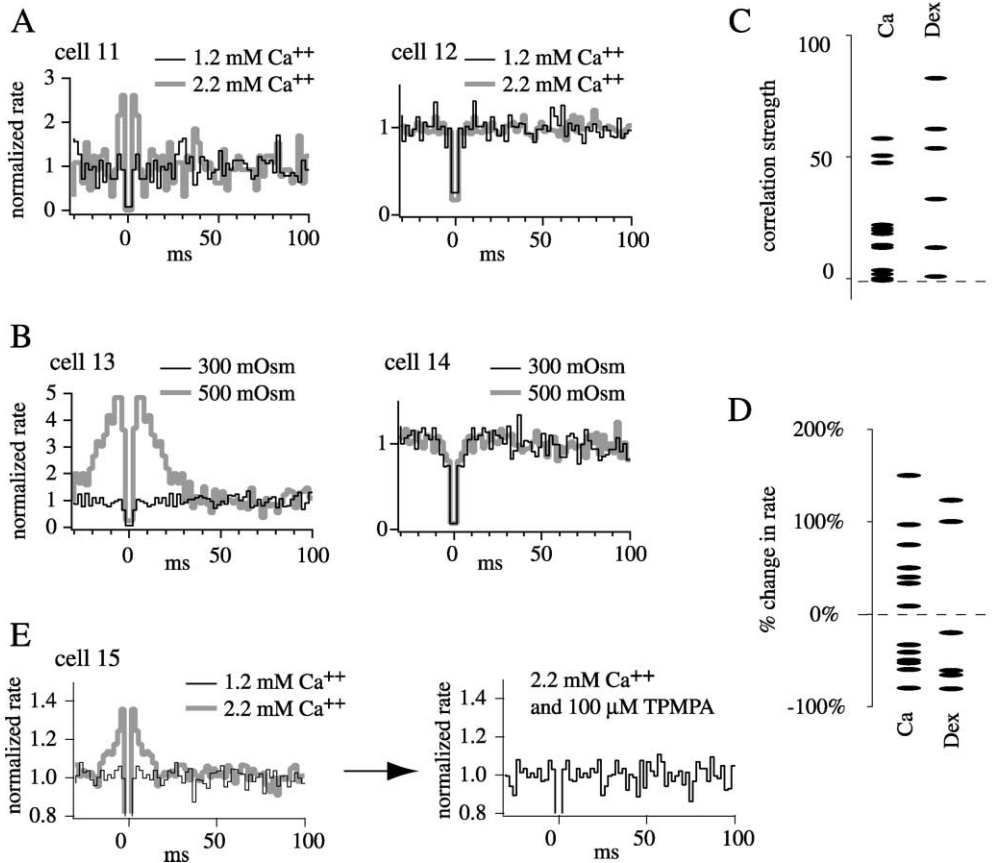
Figure 6. Increasing External Calcium or Osmolarity Induced sEPSC Correlations

(A) Increasing external Ca^{2+} induced a correlation in cell 11, but not in cell 12.

(B) Increasing external osmolarity induced a correlation in cell 13, but not in cell 14.

(C) Either manipulation usually induced a correlation, but the size of the effect varied.

(D) Raising external Ca^{2+} or osmolarity had variable effects on baseline rate.

(E) Correlation induced by raising external calcium was blocked by TPMPA.

return to standard solution, the induced correlation disappeared (n = 6/6, not shown). The strength of the induced correlation in some cells exceeded any measured in standard solution. The baseline rate declined for some cells but increased for others (Figure 6D). Thus, for cells without a correlation, augmenting synaptic transmission often induced one.

To test whether the calcium-induced correlation was caused by synaptic feedback, we chose a cell without a correlation and induced one with 2.2 mM Ca^{2+}. Then, without changing $[Ca^{2+}]$, we added 100 μM TPMPA. The antagonist completely blocked the correlation (n = 3/3 cells, Figure 6E), consistent with the idea that calcium-induced correlations depend on GABAergic feedback.

Simple Model of Feedback Circuit Replicated sEPSC Correlations

To see how a negative feedback circuit could produce a positive correlation, we constructed a simple model (Figure 7A). This included an excitatory limb, glutamate from bipolar to amacrine cell (iGluR receptor), and the two experimentally identified sources of negative

feedback, GABA from amacrine to bipolar cell ($GABA_C$ receptor) and glutamate from bipolar cell to its own metabotropic glutamate receptor (mGluR receptor). To implement the model, the bipolar cell summed a steady inward current from synaptic input (I_{input}) with quantal inhibitory currents (I_{GABA} and I_{mGluR}), represented by exponentially decaying pulses. The result was filtered by an RC circuit to produce the membrane voltage, and this set the instantaneous rate for quantal glutamate release, represented by a Poisson noise generator. Each glutamate quantum caused a quantal metabotropic current (I_{mGluR}) in the bipolar cell and a quantal excitatory current (I_{igluR}) in the amacrine cell. Within the amacrine cell, EPSCs were filtered by an RC circuit to drive quantal release of GABA.

Most of the model parameters could be given measured values. These included amplitude and decay time constant for the quantal I_{igluR} and membrane resistance and capacitance from our own recordings (I_{igluR} = 100 pS, τ_{igluR} = 6 ms, $R_{bipolar}$ = 500 MΩ, $C_{bipolar}$ = 7 pF, $R_{amacrine}$ = 340 MΩ, $C_{amacrine}$ = 8 pF). These values are similar to mean values obtained in salamander and mammalian retina in diverse experimental contexts (I_{igluR} = 130–163
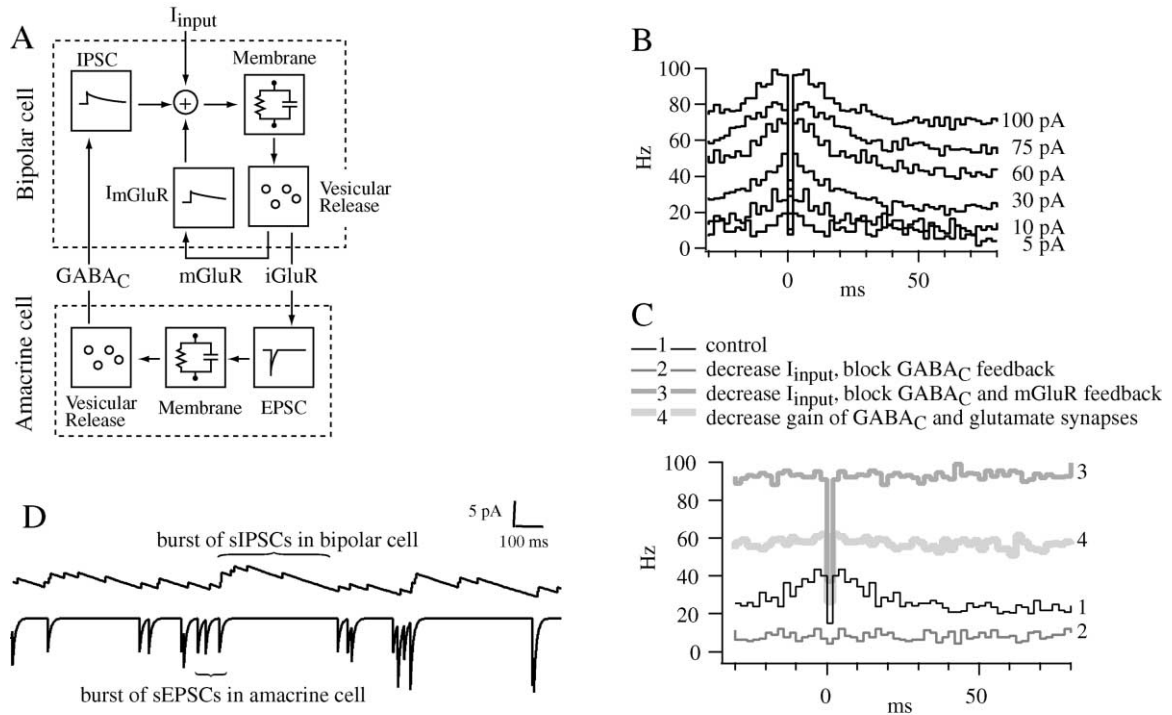
Figure 7. Computational Model of Feedback Circuit Replicated sEPSC Correlations

(A) Model of bipolar and amacrine cells in a negative feedback loop including presynaptic mGluR autoreceptors and postsynaptic iGluR and GABA$_C$ receptors (see text).

(B) Model produces correlated release despite changes in I$_{input}$ (to right of each trace).

(C) Eliminating GABA$_C$ feedback and reducing I$_{input}$ to one-tenth reduced the rate and abolished the correlation. Eliminating GABA$_C$ and mGluR feedback and reducing I$_{photo}$ to one-tenth increased the rate and abolished the correlation. Reducing gain of GABA$_C$ and glutamate synapses to one-third abolished the correlation and increased rate.

(D) Currents from bipolar cell and amacrine cell show, respectively, IPSCs and EPSCs. Note that IPSC bursts and EPSC bursts alternate.

pS, τ_{igluR} = 1–6 ms, R$_{bipolar}$ = 250–450 MΩ, C$_{bipolar}$ = 12 pF; R$_{amacrine}$ = 800 MΩ, C$_{amacrine}$ = 18 pF) (Cook and Werblin, 1994; Gao and Wu, 1999; Protti et al., 1997, 2000; Taylor et al., 1995; Tian et al., 1998). Quantal IPSCs due to GABA$_C$ have not been observed, suggesting that they are hidden by whole-cell recording noise and have amplitudes of about 1 pA; their decay time constant was taken from multiquantal currents (1.3 s) (Lukasiewicz and Shields, 1998). Synaptic delay was 1 ms (Tachibana and Okada, 1991; von Gersdorff et al., 1998). The decay time constant of I$_{mGluR}$ was 10 s (Koulen et al., 1999).

The sEPSCs in the model amacrine cell were detected automatically and used to construct an autocorrelogram. Then, the unknown parameters were adjusted until the autocorrelogram had a peak (30% correlation strength, Figure 7B). The unknown parameters were the gains (G) of glutamate and GABA synapses (i.e., release rate per membrane volts), the amplitude of I$_{mGluR}$, and the amplitude of I$_{input}$ (G$_{glutamate}$ = 60,000 quanta volts^{-1} s^{-1}, G$_{GABA}$ = 30,000 quanta volts^{-1} s^{-1}, I$_{mGluR}$ = 0.05 pA, I$_{input}$ = 30 pA). Because some measured parameters were from other experimental contexts, we tested the model's sensitivity to parameter value by increasing or decreasing each parameter in turn until the correlation strength was less than 5% or until release was too infrequent

to measure correlations. The model robustly produced correlated release across the range of physiologically reasonable values and sometimes beyond (I$_{igluR}$ = 2–3,000 pS, τ_{igluR} = 3–20,000 ms, I$_{GABA}$ = 0.3–10,000 pS, τ_{GABA} = 0.04–100 s, R$_{bipolar}$ = 500–50,000 MΩ, C$_{bipolar}$ = .03–4,000 pF, R$_{amacrine}$ = 90–9,000 MΩ, C$_{amacrine}$ = .04–300,000 pF, τ_{mGluR} = .001–100 s, synaptic delay = .02–200 ms).

The GABA$_C$ receptor might modulate current through the bipolar cell and control release rate by either of two circuits. If the receptor is present on the photoreceptor terminal (Picaud et al., 1998), a GABA$_C$ antagonist would increase the photoreceptor's release rate, decrease an inward current in the On-bipolar cell, and decrease the bipolar cell's release rate. This was the typical effect of GABA$_C$ antagonism (Figure 4D). But an Off bipolar cell would respond oppositely to GABA$_C$ antagonism and increase its release rate—which we also observed, but less frequently. If GABA$_C$ receptors were present on amacrine cells (Euler and Wassle, 1998) that constitutively inhibit a bipolar cell, GABA$_C$ antagonism would increase the inhibition of the bipolar cell and reduce its release rate. Our data did not indicate which of these possible circuits mediate the suppression of release rate by GABA$_C$ antagonists. But to test whether these circuits might suppress the correlation, we represented the

modulated bipolar cell current by I_{input} and reduced it from 100 to 5 pA (below this release was too infrequent to measure correlations). Despite striking decreases in release rate (from 80 to 10 Hz), the correlation strength actually increased (from 16% to 41%, Figure 7B). Thus, steady currents that control release rate cannot abolish the correlation.

Given a peak in the simulated autocorrelogram, all significant pharmacological effects were reproduced (Figure 7C). Blocking the GABA$_C$ synapse while reducing I_{input} abolished the correlation and decreased the rate (the typical effect of TPMPA). Blocking GABA$_C$ and mGluR synapses while reducing I_{input} abolished the correlation and raised the baseline rate (TPMPA + CPPG). Finally, decreasing the gain of both glutamate and GABA synapses abolished the correlation: this resembled (inversely) the effect of either increasing external Ca^{2+} or osmolarity.

The value of the model, beyond simulating the pharmacology of correlated release, is to illustrate how synaptic feedback synchronizes release: inhibition builds in the bipolar terminal, curtailing its release of glutamate onto the amacrine cell. As the latter stops releasing GABA, inhibition decays in the bipolar cell, which again depolarizes. This causes a burst of glutamate release, seen as EPSCs in the amacrine cell. The result is an alternation of excitatory and inhibitory bursts (Figure 7D).

Correlations Occur in the Intact Retina for Both Spontaneous and Evoked EPSCs

If correlated release is functionally significant, it should occur not only in a slice at room temperature, but also in the intact retina near body temperature. In such a preparation (see Experimental Procedures), cells had higher sEPSC rates than in the slice partly because they retained all their synaptic input. We recorded from small cells (soma diameter ≤15 μm) because their sEPSCs rates were low enough (<40 Hz) for reliable detection. These cells showed clear EPSC correlations, with an average strength of 19% ± 14% and an average duration of 45 ± 7 ms (n = 3/3, Figure 8A).

To see if EPSC correlations persisted during light responses, we stimulated the retina with sinusoidally modulated, diffuse light (see Experimental Procedures). Autocorrelograms of EPSC times were compared to the predicted autocorrelogram for a Poisson process, as calculated by a standard method for evoked events (Ghose et al., 1994; Perkel et al., 1967). Unlike the Poisson prediction for spontaneous EPSCs, which is flat because their rate is constant, the Poisson prediction for evoked EPSCs was periodically modulated by the stimulus. Half of the cells showed clear positive peaks in the autocorrelogram that were absent from the Poisson prediction (n = 3/6). The rest showed autocorrelograms that closely matched the Poisson prediction.

Correlation strength was quantified as the proportion of EPSCs in excess of that expected from a Poisson process; correlation duration was quantified as the time at which the autocorrelogram subsided into Poisson prediction (arrows in Figure 8A). Thus, correlation strength and duration for spontaneous and light-evoked EPSCs were measured identically, except that the Poisson prediction for spontaneous events was flat and for

light-driven events it was undulating. The correlation strength and duration for light-driven EPSCs averaged 14% ± 8% and 37 ± 15 ms, values similar to those for spontaneous EPSCs.

Spikes Show Temporal Correlations That Are Suppressed by TPMPA

To see if the spike statistics might reflect EPSC statistics, we again presented a sinusoidal light stimulus to the intact retina and recorded extracellularly from ganglion cells (see Experimental Procedures). We distinguished two broad classes. "Brisk" cells had a large soma (15–25 μm diameter), high capacitance (C_m ~38 pF), low resistance (R_m ~25 MΩ), and an early peaking autocorrelogram. "Sluggish" cells had a small soma (13–17 um), low capacitance (C_m ~20 pF), high resistance (R_m ~150 MΩ), and a late peaking autocorrelogram (Amthor et al., 1989; Devries and Baylor, 1997; O'Brien et al., 2002; Rockhill et al., 2002; Roska and Werblin, 2001)

For both classes, the autocorrelogram showed two clear departures from the Poisson prediction: (1) all cells showed a broad negative correlation near the origin due to a relative refractory period; (2) most sluggish cells and all brisk cells showed a positive correlation with either one or two peaks (15/17 sluggish, 7/7 brisk) (Figures 8B and 8D; Devries and Baylor, 1997; Frishman and Levine, 1983; Mastronarde, 1983; Rodieck, 1967). Sluggish cells had much broader refractory periods than brisk cells (~20 versus ~2 ms), somewhat lower correlation strengths (22% ± 20% versus 42% ± 26%), and broader correlations (37 ± 12 versus 12 ± 4 ms).

For sluggish cells, the spike correlation's duration (37 ± 12 ms) matched that of light-evoked EPSC correlations (37 ± 15 ms). If the spike correlation is caused by the EPSC correlation, it should be suppressed by antagonizing feedback onto the bipolar terminal. To test this, we recorded extracellularly from sluggish cells with positive spike correlations and applied TPMPA. In all sluggish cells tested, this suppressed the spike correlation by 50% ± 30% (n = 7/7, Figure 8B). Often, the spike rate was concomitantly decreased, presumably because TPMPA decreases ESPC rate.

After extracellular recording, we filled ganglion cells with Lucifer Yellow and identified them by morphology and stratification. Sluggish cells used for this study included types classified in rabbit as G2, G5, G6, G8, the On-Off directionally selective cell, and the local-edge detector (Amthor et al., 1989; Rockhill et al., 2002; Roska and Werblin, 2001). We recorded from enough cells to show that input/output correlations were common among sluggish cells, but the sample was insufficient to specify correlations for each type. However, one local-edge detector received correlated spontaneous and light-evoked EPSCs and three others produced spikes with a positive correlation that was blocked by TPMPA (Figures 8A and 8B).

We also selected brisk-transient cells, identified prior to recording by their large (17–25 μm) cell bodies, because their voltage fluctuations reflect quantal input with Poisson statistics (Freed, 2000). Thus, their spike correlations are unlikely to come from EPSC correlations. In agreement with this prediction, TPMPA failed to suppress the spike correlation in all four brisk-transient cells tested (2 On, 2 Off; Figure 8D).
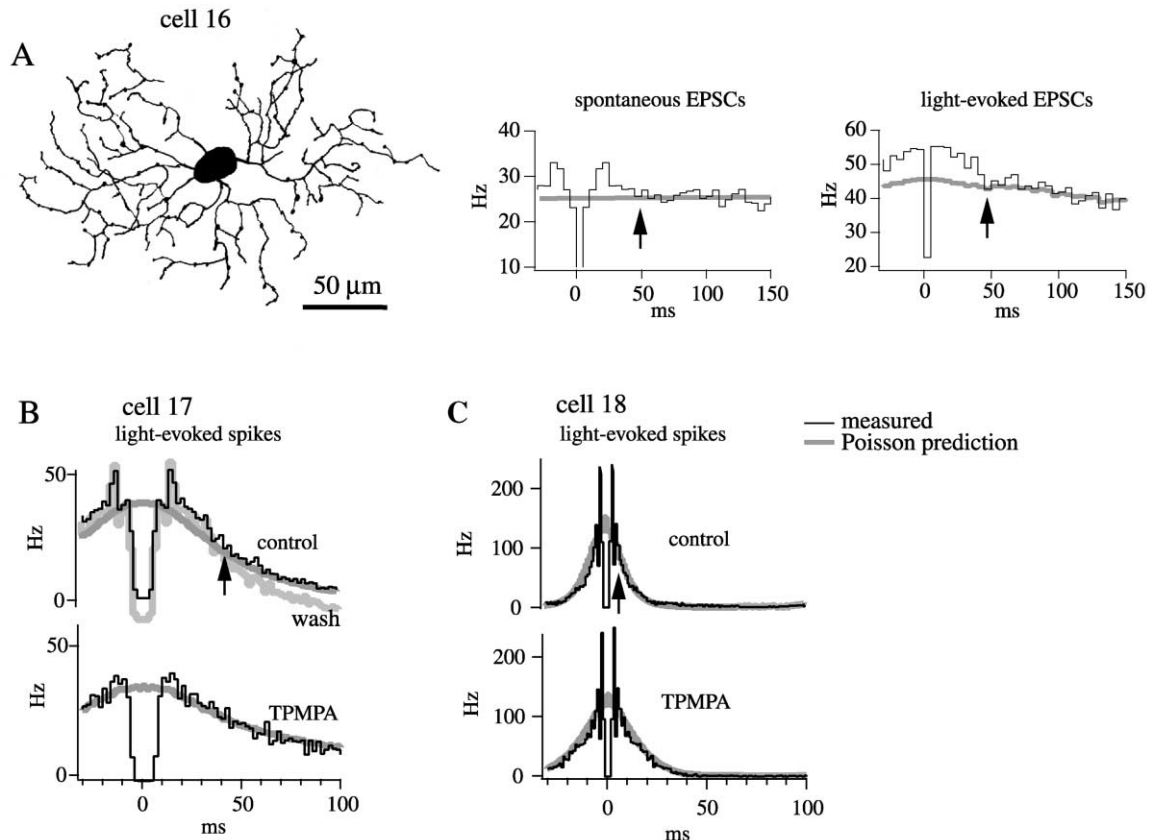
cell 16

Figure 8. EPSCs and Spikes Are Temporally Correlated in Certain Ganglion Cells

(A) Small ganglion cell (sluggish, local-edge detector) recorded in the intact retina at 34°C. For this cell, autocorrelograms of spontaneous and light-evoked EPSCs depart from a Poisson process with positive peaks lasting about 50 ms (arrows).

(B) Another local edge detector. Spiking shows two non-Poisson features: a negative notch (relative refractory period ~20 ms) and a positive peak lasting about 50 ms (arrows). The positive peak was suppressed by a $GABA_C$ antagonist.

(C) Autocorrelograms from a large ganglion cell (On brisk-transient). Its light-evoked spiking shows a non-Poisson, narrow peak lasting about 10 ms (arrow), which was not suppressed by the $GABA_C$ antagonist.

Discussion

Spontaneous Quantal Release Is Correlated by a Feedback Synapse

The retinal bipolar terminal spontaneously releases quanta in temporally correlated bursts. Bursts occurred randomly and not as oscillations because no periodicity was observed at long time scales (Figure 2B$_1$). Conceivably, sEPSCs might also show a brief negative correlation, i.e., a refractory period <3 ms, but the algorithm for detecting sEPSCs could not separate coincident or near-coincident sEPSCs. Correlated release occurs at other synapses, for example, in cerebellum, hippocampus, and neuromuscular junction, where it arises from intracellular mechanisms, such as interaction between release sites or calcium release from internal stores (Abenavoli et al., 2002; Cohen et al., 1974; Llano et al., 2000). However, the correlated release observed here appears for several reasons to be an emergent property of a local, GABAergic feedback circuit.

First, correlations are suppressed by antagonists of the $GABA_C$ receptor, which localizes on the bipolar ter-

minal postsynaptic to amacrine contacts (Figure 4; Enz et al., 1996; Koulen et al., 1998b). $GABA_C$ antagonists did not alter the average sEPSC decay time constant and only modestly reduced average sEPSC amplitude, probably by reducing the frequency of coincident quanta (Figure 5). This suggests a single population of sEPSCs whose timing is altered by synaptic feedback.

Second, correlations are induced by raising external $[Ca^{2+}]$ or osmolarity (Figure 6), manipulations that increase release probability at an isolated synapse (Fatt and Katz, 1952) and would thus increase loop gain of a feedback circuit. Correlations could be induced in some cells, suggesting that their feedback circuits normally have low loop gain. Correlations were *not* induced in other cells, suggesting that different bipolar types might vary in the strength of feedback. This is consistent with known retinal circuitry: for example, in monkey retina, midget bipolar terminals receive feedback contacts at every feedforward synapse onto an amacrine process, whereas the On S-cone bipolar terminal receives feedback contacts only rarely (Calkins and Sterling, 1996; Calkins et al., 1998). Because the medium used here

matches the ionic concentrations of retinal interstitial fluid (Ames and Nesbett, 1981; Fishman, 1980; Kaila et al., 1984), these correlations should also exist in vivo.

Third, a feedback model captures our experimental manipulations qualitatively: increasing gain in the model induces correlations, which are suppressed by blocking feedback. The model shows in principle that stochastically generated IPSCs can correlate stochastically generated EPSCs and illustrates a plausible sequence: stochastically arriving IPSCs inhibit the bipolar axon terminal. When these pause probabilistically, the bipolar terminal escapes from inhibition and releases glutamate quanta in a burst (Figure 7D). Then the burst, through the feedback loop, reestablishes inhibition and cuts itself short.

The correlations could not arise simply from fluctuations in common input to bipolar cells that contact the recorded cell. Although bipolar cells do share photoreceptor input (Cohen and Sterling, 1990b), the photon fluctuations are too small and too slow to cause the EPSC correlations (see Experimental Procedures). Nor could shared glutamate input from photoreceptors to bipolar cells cause fluctuations in bipolar cell membrane currents because these are effectively suppressed by the bright light used here (Berntson and Taylor, 2000; Euler and Masland, 2000).

Functional Implications

It is generally assumed in modeling neural circuits that quanta are released independently. If so, a circuit's signal-to-noise ratio (SNR) could be improved simply by increasing quantal rate—because for a signal carried by N quanta per unit time, the accompanying synaptic noise is proportional to $\sqrt{N}$. Thus, SNR is proportional to $N/\sqrt{N}$ (Freed et al., 1987; Manwani and Koch, 2001; Sterling et al., 1988). But here we show that quanta are actually correlated, which would render increasing quantal rate a less effective strategy (i.e., SNR $< N/\sqrt{N}$). On the other hand, synchronized quanta are more effective than independent quanta at generating a precisely timed spike, which would improve information transmission via a temporal code (Berry et al., 1997; Zador, 1998).

The local feedback circuit apparently causes the broad spike correlations found in small (sluggish) ganglion cells. The main evidence for this is that a GABA$_C$ antagonist that decorrelates quanta also decorrelates spikes, and quantal and spike correlations have similar duration ($\sim$40 ms in intact retina; Figures 8A and 8B). This differs from other instances where spike bursting arises as an intrinsic property of one neuron, which is then amplified and/or further synchronized by synaptic circuitry (Hammond, 2001; Koch, 1999; Larkum et al., 2001; Llinas and Yarom, 1981; McCormick and Contreras, 2001; Spencer and Kandel, 1968). The feedback mechanism does not cause the spike correlations of brisk-transient cells, which are unaffected by GABA$_C$ antagonism; nor is it responsible for the spontaneous spike bursts of immature mammalian ganglion cells (Masland, 1977; Meister et al., 1991; Sernagor and Grzywacz, 1996), which start before bipolar synapses are formed and later depend on GABA$_A$ not GABA$_C$ receptors (Feller et al., 1996; Fischer et al., 1998; Wong et al., 2000).

The GABA$_C$ IPSC seems well suited to correlate spikes in a sluggish cell because it is so prolonged. Its decay time constant is about 10-fold longer than that of GABA$_A$ and glycine IPSCs (Frech et al., 2001; Lukasiewicz and Shields, 1998; Protti et al., 1997; Tian et al., 1998). Because a receptor mediating negative feedback subtracts out signal frequencies below its own characteristic frequency, the GABA$_C$ receptor passes lower frequencies than a GABA$_A$ receptor and thus allows a greater bandwidth. Thus, the GABA$_C$ receptor's low characteristic frequency seems suited to the sluggish cell's slow visual response (maximum at $\sim$1 Hz versus $\sim$10 Hz for brisk cells) (Cleland and Levick, 1974; Frishman et al., 1987; Troy et al., 1989).

Recordings

From an adult Hartley guinea pig (400–600 gm, >8 wks) anesthetized with ketamine (133 mg kg^{-1}), xylazine (13 mg kg^{-1}), and pentobarbital (100 mg kg^{-1}), an eye was removed, following which the animal was killed by anesthetic overdose. All procedures were performed in accordance with University of Pennsylvania and National Institutes of Health guidelines. Retinal slices and pieces of intact retina were mounted in a chamber on an upright microscope with infrared differential interference contrast optics (Protti et al., 1997; Tian et al., 1998; Werblin, 1978; Zhou, 1998). A light-emitting diode, driven by a digital-to-analog converter, evenly illuminated the preparation (10^6 photon μm^{-2} s^{-1}, 560 nm). For visual stimulation, the light intensity was sinusoidally modulated by 5%–20% (2–4 Hz for brisk cells, 1–2 Hz for sluggish, 100 repeats of 8–10 s each). The tissue was superfused with Ames' medium (Sigma), which was saturated with 5% CO$_2$/95% O$_2$ and adjusted with glucose to $\sim$300 mOsm and contained (in mM) 120 NaCl, 3.1 KCl, 0.5 KH$_2$PO$_4$, 23 Na$_2$HCO$_3$, 1.2 Mg$_2$SO$_4$, 1.15 CaCl$_2$, plus amino acids and vitamins. To substitute Ca^{2+} for Mg^{2+} without altering any other ionic concentration, we omitted amino acids and vitamins from the control solution. This solution was changed to one adjusted to equal osmolarity with glucose and composed of (in mM) 118 NaCl, 3.1 KCl, 0.5 KH$_2$PO$_4$, 23.5 Na$_2$HCO$_3$, 0.2 Mg$_2$SO$_4$, 2.15 CaCl$_2$, 1 NaSO$_4$.

Patch electrodes (12 MΩ) were filled with (in mM) 140 Cs gluconate, 1 CaCl$_2$, 1 MgCl$_2$, 5 EGTA, 10 HEPES (310 mOsm). In experiments on intact retina, this solution was supplemented with 0.3% Lucifer Yellow. The calculated reversal potential for glutamate channels, with equal permeability to Cs$^+$ and Na$^+$, was about 0 mV, and the calculated reversal potential for Cl$^-$ channels (GABA, glycine) was about −87 mV. All voltages were corrected for a calculated junction potential of 15 mV. The recordings were acquired with an AxoPatch 200B patch clamp amplifier (8-pole Bessel filter, f$_c$ = 1 kHz) and digitized online at 5 kHz using pClamp 7 (Axon Instruments). Voltage-clamp recordings were performed in whole-cell mode and were selected for a time constant (access resistance $\times$ cell capacitance) of <300 μs. The holding voltage was set to the Cl$^-$ equilibrium potential to null out spontaneous IPSCs. Contamination by IPSCs was insignificant for several reasons: (1) all detectable spontaneous currents (i.e., >3 pA) were blocked with the glutamate receptor antagonist 6-cyano-7-nitroquinoxaline-2,3-dione (CNQX, 50 μM, n = 3 cells); (2) although the cell might experience a membrane potential positive to the holding voltage due to voltage drops across the dendrites' axial resistance and the pipette's access resistance (30 MΩ), the resulting outward currents (sIPSCs) would be ignored by the detection algorithm; and (3) the cumulative frequency distributions of amplitude and time constant were uninflected, and when plotted as histograms had single modes, indicating a single population of PSCs (Figure 5). Extracellular recordings were performed in tight-seal current clamp mode. After recording, Lucifer-filled cells were photographed with a cooled-CCD camera (Hamamatsu).

Analysis

Recordings were analyzed offline using IGOR (Wavemetrics). An interval (200–300 s) that contained 1500–6000 identifiable EPSCs

was used for each condition (control, experimental, wash). The "peak location" algorithm smoothed the recording (1 ms) and found a local maximum (the leading edge) followed by a local minimum (the peak) followed by an exponential decay (criterion R^2 for exponential = 0.7) (Tian et al., 1998). Threshold EPSC amplitude was typically set at 3 pA to exceed the peak-to-peak noise level between EPSCs (<0.8 pA). A template matching algorithm (Clements and Bekkers, 1997) was also tried, but it detected overlapping sEPSCs at short intervals less reliably and thus produced a wider artifactual notch in the autocorrelogram.

As EPSC rate increased, EPSCs coincided more often, which reduced the detection algorithm's reliability. This slightly decreased the measured correlation strength. To gauge the magnitude of this effect, we constructed shuffled recordings by modulating the mean rate of the Poisson process with random exponential pulses ($\tau = 4$ ms) to cause positive correlations between EPSCs (n = 6 cells). By varying the baseline rate of these shuffled recordings, we found that correlation strength declined by an average of 0.8% for each 1 Hz increase in baseline rate. We corrected for this effect in drug experiments by subtracting the expected change in correlation strength due solely to a change in baseline rate from the measured changes in correlation strength due to an antagonist. The corrections were small (1% ± 5%) compared to the magnitude of measured antagonist effects (52% ± 8%).

The Poisson prediction for the autocorrelogram of light-driven events was constructed by a standard method (Ghose et al., 1994), by constructing a histogram of average spike counts over repeated trials (PSTH) and computing its autocorrelation. This is equivalent to forming a crosscorrelation between every trial and every *other* trial ("shift predictor") (Perkel et al., 1967).

The photon fluctuations during steady illumination (which proved to be negligible) were calculated as follows: 5×10^5 photons $\mu m^{-2} s^{-1}$, 560 nm (60% bleach) caused within a cone outer segment about 2×10^5 photon absorptions s^{-1} ($\lambda_{max} \approx 530$ nm for superior retina) (Jacobs and Deegan, 1994; Parry and Bowmaker, 2002; Rohlich et al., 1994) (for calculation method, see Freed, 2000). Since at least five cones converge upon a bipolar cell by chemical synapses (Cohen and Sterling, 1990b) and many more through electrical synapses, the bipolar cell receives signals from at least 1×10^6 photon absorptions s^{-1}, or about 1×10^5 in the photoreceptor's 100 ms integration time. Because photon absorptions are Poisson, this mean rate implies a signal-to-noise ratio of more than 300. Consequently, photon fluctuations were too small to correlate the quantal release from bipolar cells. Consistent with this, the correlations measured here are on average too brief (18 ms in amacrine cells) to result from single photon responses in photoreceptors which last about 100 ms (Baylor et al., 1984).

References

Abenavoli, A., Forti, L., Bossi, M., Bergamaschi, A., Villa, A., and Malgaroli, A. (2002). Multimodal quantal release at individual hippocampal synapses: evidence for no lateral inhibition. J. Neurosci. *22*, 6336–6346.

Ames, A., and Nesbett, F.B. (1981). In vitro retina as an experimental model of the central nervous system. J. Neurochem. *37*, 867–877.

Amthor, F.R., Takahashi, E.S., and Oyster, C.W. (1989). Morphologies of rabbit retinal ganglion cells with complex receptive fields. J. Comp. Neurol. *280*, 97–121.

Awatramani, G.B., and Slaughter, M.M. (2001). Intensity-dependent,

rapid activation of presynaptic metabotropic glutamate receptors at a central synapse. J. Neurosci. *21*, 741–749.

Barrett, E.F., and Stevens, C.F. (1972). Quantal independence and uniformity of presynaptic release kinetics at the frog neuromuscular junction. J. Physiol. *227*, 665–689.

Baylor, D.A., Nunn, B.J., and Schnapf, J.L. (1984). The photocurrent, noise and spectral sensitivity of rods of the monkey *Macaca Fascicularis*. J. Physiol. *357*, 575–607.

Berntson, A., and Taylor, W.R. (2000). Response characteristics and receptive field widths of on-bipolar cells in the mouse retina. J. Physiol. *524*, 879–889.

Berry, M.J., Warland, D.K., and Meister, M. (1997). The structure and precision of retinal spike trains. Proc. Natl. Acad. Sci. USA *94*, 5411–5416.

Bornstein, J.C. (1978). Spontaneous multiquantal release at synapses in guinea-pig hypogastric ganglia: evidence that release can occur in bursts. J. Physiol. *282*, 375–398.

Calkins, D.J., and Sterling, P. (1996). Absence of spectrally specific lateral inputs to midget ganglion-cells in primate retina. Nature *381*, 613–615.

Calkins, D.J., Tsukamoto, Y., and Sterling, P. (1998). Microcircuitry and mosaic of a blue-yellow ganglion cell in the primate retina. J. Neurosci. *18*, 3373–3385.

Chebib, M., Mewett, K.N., and Johnston, G.A. (1998). GABA(C) receptor antagonists differentiate between human rho1 and rho2 receptors expressed in *Xenopus* oocytes. Eur. J. Pharmacol. *357*, 227–234.

Cleland, B.G., and Levick, W.R. (1974). Brisk and sluggish concentrically organized ganglion cells in the cat's retina. J. Physiol. *240*, 421–456.

Clements, J.D., and Bekkers, J.M. (1997). Detection of spontaneous synaptic events with an optimally scaled template. Biophys. J. *73*, 220–229.

Cohen, E., and Sterling, P. (1990a). Demonstration of cell types among cone bipolar neurons of cat retina. Philos. Trans. R. Soc. Lond. B Biol. Sci. *330*, 305–321.

Cohen, E., and Sterling, P. (1990b). Convergence and divergence of cones onto bipolar cells in the central area of cat retina. Philos. Trans. R. Soc. Lond. B Biol. Sci. *330*, 323–328.

Cohen, I., Kita, H., and van der Kloot, W. (1974). The stochastic properties of spontaneous quantal release of transmitter at the frog neuromuscular junction. J. Physiol. *236*, 341–361.

Cook, P.B., and Werblin, F.S. (1994). Spike initiation and propagation in wide field transient amacrine cels of the salamander retina. J. Neurosci. *14*, 3852–3861.

de Ruyter van Steveninck, R.R., Lewen, G.D., Strong, S.P., Koberle, R., and Bialek, W. (1997). Reproducibility and variability in neural spike trains. Science *275*, 1805–1808.

Del Castillo, J., and Katz, B. (1954). Quantal components of the endplate potential. J. Physiol. *124*, 560–573.

Demb, J.B., Haarsma, L., Freed, M.A., and Sterling, P. (1999). Functional circuitry of the retinal ganglion cell's nonlinear receptive field. J. Neurosci. *19*, 9756–9767.

Devries, S.H., and Baylor, D.A. (1997). Mosaic arrangement of ganglion cell receptive fields in rabbit retina. J. Neurophysiol. *78*, 2048–2060.

Enz, R., Brandstatter, J.H., Wässle, H., and Bormann, J. (1996). Immunocytochemical localization of the Gaba(C) receptor rho-subunits in the mammalian retina. J. Neurosci. *16*, 4479–4490.

Euler, T., and Masland, R.H. (2000). Light-evoked responses of bipolar cells in a mammalian retina. J. Neurophysiol. *83*, 1817–1829.

Euler, T., and Wassle, H. (1998). Different contributions of GABAA and GABAC receptors to rod and cone bipolar cells in a rat retinal slice preparation. J. Neurophysiol. *79*, 1384–1395.

Fatt, P., and Katz, B. (1952). Spontaneous subthreshold activity at motor nerve endings. J. Physiol. *117*, 109–128.

Feller, M.B., Wellis, D.P., Stellwagen, D., Werblin, F.S., and Shatz, C.J. (1996). Requirement for cholinergic synaptic transmission in

the propagation of spontaneous retinal waves. Science *0272*, 1182–1187.

Fischer, K.F., Lukasiewicz, P.D., and Wong, R.O. (1998). Age-dependent and cell class-specific modulation of retinal ganglion cell bursting activity by GABA. J. Neurosci. *18*, 3767–3778.

Fishman, R.H. (1980). Cerebrospinal fluid in diseases of the nervous system (Philadelphia: Saunders).

Fletcher, E.L., and Wassle, H. (1999). Indoleamine-accumulating amacrine cells are presynaptic to rod bipolar cells through GABA(c) receptors. J. Comp. Neurol. *413*, 155–167.

Frech, M.J., Perez-Leon, J., Wassle, H., and Backus, K.H. (2001). Characterization of the spontaneous synaptic activity of amacrine cells in the mouse retina. J. Neurophysiol. *86*, 1632–1643.

Freed, M.A. (2000). Rate of quantal excitation to a retinal ganglion cell evoked by sensory input. J. Neurophysiol. *83*, 2956–2966.

Freed, M., Smith, R., and Sterling, P. (1987). Rod bipolar array in the cat retina: pattern of input from rods and GABA-accumulating amacrine cells. J. Comp. Neurol. *266*, 445–455.

Frishman, L.J., and Levine, M.W. (1983). Statistics of the maintained discharge of cat retinal ganglion cells. J. Physiol. *339*, 475–494.

Frishman, L.J., Freeman, A.W., Troy, J.B., Shweitzer-Tong, D.E., and Enroth-Cugell, C. (1987). Spatiotemporal frequency responses of cat retinal ganglion cells. J. Gen. Physiol. *89*, 599–627.

Gao, F., and Wu, S.M. (1999). Multiple types of spontaneous excitatory synaptic currents in salamander retinal ganglion cells. Brain Res. *821*, 487–502.

Ghose, G.M., Ohzawa, I., and Freedman, R.D. (1994). Receptive-field maps of correlated discharge between pairs of neurons in the cat's visual cortex. J. Neurophysiol. *71*, 330–346.

Grunert, U., and Wassle, H. (1993). Immunocytochemical localization of glycine receptors in the mammalian retina. J. Comp. Neurol. *335*, 523–537.

Hammond, C. (2001). Cellular and Molecular Neurobiology, second edition (San Diego, CA: Academic Press).

Hartveit, E. (1999). Reciprocal synaptic interactions between rod bipolar cells and amacrine cells in the rat retina. J. Neurophysiol. *81*, 2923–2936.

Jacobs, G.H., and Deegan, J.F. (1994). Spectral sensitivity, photo-topigments, and color vision in the guinea pig (*Cavia porcellus*). Behav. Neurosci. *108*, 993–1004.

Kaila, K., Voipio, J., and Akerman, K.E. (1984). Free extracellular [Ca2+] at photoreceptor level equals that in vitreous in frog and carp eyes. Invest. Opthalmol. Vis. Sci. *25*, 1395–1401.

Kara, P., Reinagel, P., and Reid, R.C. (2000). Low response variability in simultaneously recorded retinal, thalamic, and cortical neurons. Neuron *27*, 635–646.

Koch, C. (1999). Computational Neuroscience (Oxford: Oxford University Press).

Koulen, P., Brandstatter, J.H., Enz, R., Bormann, J., and Wassle, H. (1998a). Synaptic clustering of GABA(C) receptor rho-subunits in the rat retina. Eur. J. Neurosci. *10*, 115–127.

Koulen, P., Brandstatter, J.H., Enz, R., Bormann, J., and Wässle, H. (1998b). Synaptic clustering of GABA(C) receptor rho-subunits in the rat retina. Eur. J. Neurosci. *10*, 115–127.

Koulen, P., Kuhn, R., Wassle, H., and Brandstatter, J.H. (1999). Modulation of the intracellular calcium concentration in photoreceptor terminals by a presynaptic metabotropic glutamate receptor. Proc. Natl. Acad. Sci. USA *96*, 9909–9914.

Larkum, M.E., Zhu, J.J., and Sakmann, B. (2001). Dendritic mechanisms underlying the coupling of the dendritic with the axonal action potential initiation zone of adult rat layer 5 pyramidal neurons. J. Physiol. *533*, 447–466.

Llano, I., Gonzalez, J., Caputo, C., Lai, F.A., Blayney, L.M., Tan, Y.P., and Marty, A. (2000). Presynaptic calcium stores underlie large-amplitude miniature IPSCs and spontaneous calcium transients. Nat. Neurosci. *3*, 1256–1265.

Llinas, R., and Yarom, Y. (1981). Electrophysiology of mammalian inferior olivary neurones in vitro. Different types of voltage-dependent ionic conductances. J. Physiol. *315*, 549–567.

Lukasiewicz, P.D., and Shields, C.R. (1998). Different combinations of GABA(A) and GABA(C) receptors confer distinct temporal properties to retinal synaptic responses. J. Neurophysiol. *79*, 3157–3167.

Manwani, A., and Koch, C. (2001). Detecting and estimating signals over noisy and unreliable synapses: information-theoretic analysis. Neural Comput. *13*, 1–33.

Marty, A., and Neher, E. (1995). Tight-seal whole-cell recording. In Single Channel Recording, B. Sakmann and E. Neher, eds. (New York: Plenum Press), pp. 31–52.

Masland, R.H. (1977). Maturation of function in the developing rabbit retina. J. Comp. Neurol. *175*, 275–286.

Mastronarde, D.N. (1983). Correlated firing of cat retinal ganglion cells. II. Responses of X- and Y-cells to single quantal events. J. Neurophysiol. *49*, 325–349.

McCormick, D.A., and Contreras, D. (2001). On the cellular and network bases of epileptic seizures. Annu. Rev. Physiol. *63*, 815–846.

McGillem, G.S., Rotolo, T.C., and Dacheux, R.F. (2000). GABA responses of rod bipolar cells in rabbit retinal slices. Vis. Neurosci. *17*, 381–389.

Meister, M., and Berry, M.J. (1999). The neural code of the retina. Neuron *22*, 435–450.

Meister, M., Wong, R.O., Baylor, D.A., and Shatz, C.J. (1991). Synchronous bursts of action potentials in ganglion cells of the developing mammalian retina. Science *252*, 939–943.

O'Brien, B.J., Isayama, T., Richardson, R., and Berson, D.M. (2002). Intrinsic physiological properties of cat retinal ganglion cells. J. Physiol. *538*, 787–802.

Parry, J.W., and Bowmaker, J.K. (2002). Visual pigment coexpression in guinea pig cones: a microspectrophotometric study. Invest. Ophthalmol. Vis. Sci. *43*, 1662–1665.

Perkel, D.H., Gerstein, G.L., and Moore, G.P. (1967). Neuro spike trains and stochastic point processes II. Simultaneous spike trains. J. Neurophysiol. *7*, 419–440.

Picaud, S., Pattnaik, B., Hicks, D., Forster, V., Fontaine, V., Sahel, J., and Dreyfus, H. (1998). GABAA and GABAC receptors in adult porcine cones: evidence from a photoreceptor-glia co-culture model. J. Physiol. *513*, 33–42.

Protti, D.A., Gerschenfeld, H.M., and Llano, I. (1997). GABAergic and glycinergic IPSCs in ganglion cells of rat retinal slices. J. Neurosci. *17*, 6075–6085.

Protti, D.A., Flores-Herr, N., and von Gersdorff, H. (2000). Light evokes Ca2+ spikes in the axon terminal of a retinal bipolar cell. Neuron *25*, 215–227.

Rockhill, R.L., Daly, F.J., MacNeil, M.A., Brown, S.P., and Masland, R.H. (2002). The diversity of ganglion cells in a mammalian retina. J. Neurosci. *22*, 3831–3843.

Rodieck, R.W. (1967). Maintained activity of cat retinal ganglion cells. J. Neurophysiol. *30*, 1043–1071.

Rohlich, P., van Veen, T., and Szel, A. (1994). Two different visual pigments in one retinal cone cell. Neuron *13*, 1159–1166.

Roska, B., and Werblin, F. (2001). Vertical interactions across ten parallel, stacked representations in the mammalian retina. Nature *410*, 583–587.

Sernagor, E., and Grzywacz, N.M. (1996). Influence of spontaneous activity and visual experience on developing retinal receptive-fields. Curr. Biol. *6*, 1503–1508.

Spencer, W.A., and Kandel, E.R. (1968). Cellular and integrative properties of the hippocampal pyramidal cell and the comparative electrophysiology of cortical neurons. Int. J. Neurol. *6*, 266–296.

Sterling, P., Freed, M.A., and Smith, R.G. (1988). Architecture of rod and cone circuits to the On-beta ganglion cell. J. Neurosci. *8*, 623–642.

Stevens, C.F. (1993). Quantal release of neurotransmitter and long-term potentiation. Cell *72*, 55–63.

Tachibana, M., and Okada, T. (1991). Release of endogenous excit-

atory amino acids from on-type bipolar cells isolated from the gold-fish retina. J. Neurosci. *11*, 2199–2208.

Taylor, W.R., Chen, E., and Copenhagen, D.R. (1995). Characterization of spontaneous excitatory synaptic currents in salamander retinal ganglion cells. J. Physiol. *486*, 207–221.

Tian, N., Hwang, T.N., and Copenhagen, D.R. (1998). Analysis of excitatory and inhibitory spontaneous synaptic activity in mouse retinal ganglion cells. J. Neurophysiol. *80*, 1327–1340.

Troy, J., Einstein, G., Schuurmans, R., Robson, J., and Enroth-Cugell, C. (1989). Responses to sinusoidal gratings of 2 types of very nonlinear retinal ganglion cells of cat. Vis. Neurosci. *3*, 213–223.

Tsukamoto, Y., Morigiwa, K., Ueda, M., and Sterling, P. (2001). Microcircuits for night vision in mouse retina. J. Neurosci. *21*, 8616–8623.

von Gersdorff, H., Sakaba, T., Berglund, K., and Tachibana, M. (1998). Submillisecond kinetics of glutamate release from a sensory synapse. Neuron *21*, 1177–1188.

Werblin, F.S. (1978). Transmission along and between rods in the tiger salamander retina. J. Physiol. *280*, 449–470.

Wong, W.T., Myhr, K.L., Miller, E.D., and Wong, R.O. (2000). Developmental changes in the neurotransmitter regulation of correlated spontaneous retinal activity. J. Neurosci. *20*, 351–360.

Zador, A. (1998). Impact of synaptic unreliability on the information transmitted by spiking neurons. J. Neurophysiol. *79*, 1219–1229.

Zhou, Z.J. (1998). Direct participation of starburst amacrine cells in spontaneous rhythmic activities in the developing mammalian retina. J. Neurosci. *18*, 4155–4165.